Charge screening effect on hadron-quark mixed phase in compact stars

Tomoki Endo[*]

Department of Physics, Kyoto University, Kyoto 606-8502, Japan
E-mail: endo@ruby.scphys.kyoto-u.ac.jp

Toshiki Maruyama

Japan Atomic Energy Research Institute,[†] *Tokai, Ibaraki 319-1195, Japan*
E-mail: maruyama.toshiki@jaea.go.jp

Satoshi Chiba

Japan Atomic Energy Research Institute,[†] *Tokai, Ibaraki 319-1195, Japan*
E-mail: chiba.satoshi@jaea.go.jp

Toshitaka Tatsumi

Department of Physics, Kyoto University, Kyoto 606-8502, Japan
E-mail: tatsumi@ruby.scphys.kyoto-u.ac.jp

We study the charge screening effect in the hadron-quark mixed phase. By including the charge screening effect, rearrangement of charged particles occurs and some part becomes locally charge-neutral. As a result the equation of state for the mixed phase becomes close to that given by the Maxwell construction, which means that the Maxwell construction would effectively gain the physical meaning again even in the system with two or more chemical potentials. We also discuss the interplay of the surface tension and the Coulomb interaction. Both effects would restrict the region of the mixed phase in the core of hybrid stars.

29th Johns Hopkins Workshop on current problems in particle theory: strong matter in the heavens
1-3 August
Budapest

---

[*]Speaker.

[†]Present name: Japan Atomic Energy Agency

1. Introduction

It is widely believed that quark matter exists in high-temperature and/or high-density situations like in the relativistic heavy-ion collisions (RHIC) [1] or in the core of neutron stars [2, 3], and the "deconfinement transition" has been actively searched. Theoretical studies using model calculations or based on the first principle, lattice QCD [4] have been also carried out by many authors to find the critical temperature. Although many exciting results have been reported, the deconfinement transition has not been clearly understood yet.

We, hereafter, consider the phase transition from hadron phase to three-flavor quark phase in neutron-star matter in a semi-phenomenological way. Since many theoretical calculations have suggested that the deconfinement transition should be of first order in low-temperature and high-density area [5, 6], we assume the first-order phase transition in this paper. If the deconfinement transition is of first order, one may expect a *mixed phase* during the transition. Actually, the hadron-quark mixed phase has been considered during the hadronization era in RHIC [7, 8, 9] or in the core region of neutron stars [10, 11, 12].

There is an issue about the mixed phase for the first-order phase transitions with two or more chemical potentials [13]. We often use the Maxwell construction (MC) to derive the equation of state (EOS) in thermodynamic equilibrium, as in the liquid-vapor phase transition of water, where both phases consist of single particle species. However, if many particle species participate in the phase transition as in neutron-star matter, MC is no more an appropriate method. Before Glendenning first pointed out [13], many people have applied MC to get EOS for the first-order phase transitions [14, 15, 16, 17] expected in neutron stars, such as pion or kaon condensation and the deconfinement transition.

Let us consider a deconfinement transition in neutron-star matter. We must introduce many chemical potentials for particle species, but the independent ones in this case are reduced to two, i.e. baryon-number chemical potential μ_B and charge chemical potential μ_Q, due to chemical equilibrium and total charge neutrality. They are nothing but the neutron and electron chemical potentials, μ_n and μ_e, respectively. In the mixed-phase these chemical potentials should be spatially constant. When we naively apply MC to get EOS in thermodynamic equilibrium, we immediately notice that μ_B is constant in the mixed-phase, while μ_e is different in each phase because of the difference of the electron number density in these phases. This is because MC uses EOS of bulk matter in each phase, which is of locally charge-neutral and uniform matter; many electrons are needed in hadron matter to compensate the positive charge of protons, while in quark matter charge neutrality is almost fulfilled without electrons. Thus

$$\mu_B^Q = \mu_B^H, \quad \mu_e^Q \neq \mu_e^H, \tag{1.1}$$

in MC, where superscripts "Q" and "H" denote the quark and hadron phases, respectively. Glendenning emphasized that we must use the Gibbs conditions (GC) in this case instead of MC, which relaxes the charge-neutrality condition to be globally satisfied as a whole, not locally in each phase [13]. GC imposes the following conditions,

$$\mu_B^Q = \mu_B^H, \quad \mu_e^Q = \mu_e^H,$$
$$P^Q = P^H, \quad T^Q = T^H. \tag{1.2}$$

He demonstrated a wide region of the mixed phase, where two phases have a net charge but totally charge-neutral: EOS thus obtained, different from that given by MC, never exhibits a constant-pressure region. He simply considered a mixed phase consisting of two bulk matters separated by a sharp boundary without any surface tension and the Coulomb interaction, which we call "bulk Gibbs" for convenience. "Bulk Gibbs" requires that each matter can have a net charge but the total charge is neutral,

$$f_V \rho_{\text{ch}}^{\text{Q}} + (1 - f_V)\rho_{\text{ch}}^{\text{H}} = 0, \tag{1.3}$$

where f_V means the volume fraction of quark matter in the mixed phase and "$\rho_{\text{ch}}^{\text{Q,H}}$" means charge density in each matter. Figure 1 shows the phase diagram in the μ_{B} - μ_e plane. We can see that there is a discontinuous jump in μ_e for the case of MC, while the curve given by "bulk Gibbs" smoothly connects uniform hadron matter and uniform quark matter; the mixed phase can appear in a wide μ_{B} region in "bulk Gibbs", in contrast with MC [18].
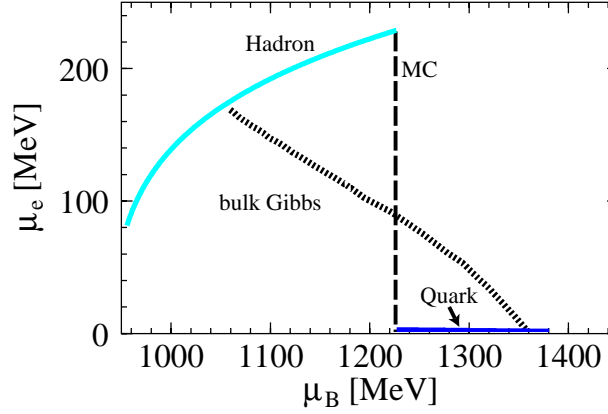

Figure 1: Phase diagram in the $\mu_{\text{B}} - \mu_e$ plane. There appears no region of the mixed phase by the calculation with MC, while a wide region of the mixed phase by the 'bulk Gibbs' calculation.

However, this "bulk Gibbs" is too simple to study the mixed phase, since we must consider matter with non-uniform structures instead of two bulk uniform matters; the mixed phase should have various geometrical structures where both the number and charge densities are no more uniform. Then we have to take into account finite-size effects like the surface and the Coulomb interaction energies. We show that the mixed phase should be narrow in the μ_{B} space by the charge screening effect, and derive EOS for the deconfinement transition in neutron-star matter. We shall see EOS results in being similar to that given by MC. We also discuss the interplay of the Coulomb interaction effect and the surface effect in the context of the hadron-quark mixed phase. Preliminary results for the droplet case has been already reported in Ref. [19].

2. Brief review of the previous works

Heiselberg et al. [20] studied a geometrical structure in the mixed phase by considering the spherical quark droplets embedded in hadron matter. They introduced the surface tension and treated its strength as a free parameter because the surface tension at the hadron-quark interface

has not been clearly understood. They pointed out that if the surface tension parameter σ is large ($\sigma \geq 90$ MeV/fm^2), the region of the mixed phase is largely limited or cannot exist. Subsequently
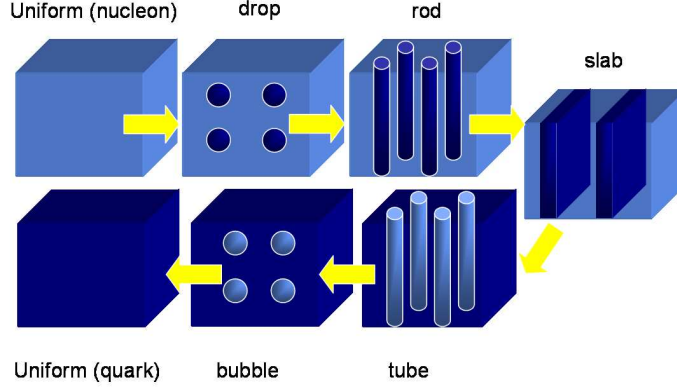

Figure 2: Schematic image of structured mixed phase.

Glendenning and Pei [10] have suggested "crystalline structures of the mixed phase" which have some geometrical structures, "droplet", "rod", "slab", "tube", and "bubble" (Fig. 2), assuming a small σ[10, 21]. The finite-size effects are obvious in these calculations by observing energies. We may consider only a single cell, by dividing the whole space into equivalent Wigner-Seitz cells: the cell size is denoted by R_W and the size of the lump (droplet, rod, slab, tube or bubble) by R (Fig. 3). Then the surface energy density is expressed in terms of the surface tension parameter σ as

$$\varepsilon_S = \frac{f_V \sigma d}{R}, \tag{2.1}$$

where d denotes the dimensionality of each geometrical structure; $d = 3$ for droplet and bubble, $d = 2$ for rod and tube, and $d = 1$ for slab. The Coulomb energy density reads

$$\varepsilon_C = 2\pi e^2 \left(\rho_{\text{ch}}^{\text{H}} - \rho_{\text{ch}}^{\text{Q}} \right)^2 R^2 \Phi_d(f_V) , \tag{2.2}$$

$$\Phi_d(f_V) \equiv \left[2(d-2)^{-1} \left(1 - \frac{1}{2} d f_V^{1-2/d} \right) + f_V \right] (d+2)^{-1}, \tag{2.3}$$

where we simply assume an uniform density distribution in each phase. When we minimize the sum of ε_S and ε_C with respect to the size R for a given volume fraction f_V, we can get the well-known relation,

$$\varepsilon_S = 2\varepsilon_C. \tag{2.4}$$

This implies that an optimal size of the lump is determined by the balance of these finite-size effects. Eventually we can express the sum of the surface and Coulomb energy densities with an optimal cell size [20]:

$$\varepsilon_C^{(d)} + \varepsilon_S^{(d)} = 3 f_V d \left(\frac{\pi \sigma^2 \left(\rho_{\text{ch}}^{\text{H}} - \rho_{\text{ch}}^{\text{Q}} \right)^2 \Phi_d(f_V)}{2d} \right)^{1/3} . \tag{2.5}$$

Thus we can calculate the energy of any geometrically structured mixed phase with (2.5) by changing the parameter d. Many authors have taken this treatment for the mixed phase[10, 18, 20]. Note that the energy sum in Eq. (2.5) becomes larger as the surface tension gets stronger, while the relation Eq.(2.4) is always kept.
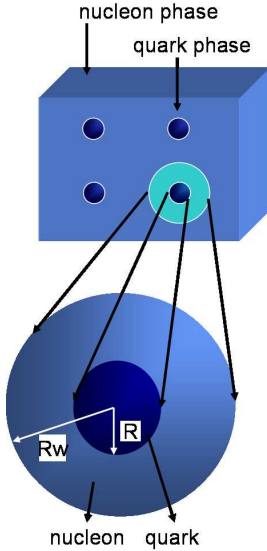

nucleon phase

quark phase

R_W

R

nucleon   quark

Figure 3: Wigner-Seitz approximation for the droplet case. R is the droplet radius and R_W the cell radius.

However, this treatment is not a self-consistent but a perturbative one, since the charge screening effect for the Coulomb potential or the rearrangement effect of charged-particles in the presence of the Coulomb interaction is completely discarded. We shall see that the Coulomb potential is never weak in the mixed phase, and thereby this treatment overestimates the Coulomb energy. The charge screening effect is included only if we introduce the Coulomb potential and consistently solve the Poisson equation with other equations of motion for charged particles. Consequently it is a highly non-perturbative effect. Norsen and Reddy [22] have studied the Debye screening effect in the context of kaon condensation to see a large change of the charged-particle densities like kaons and protons. Maruyama et al. have numerically studied it in the context of liquid-gas phase transition at subnuclear densities [23], where nuclear pasta can be regarded as geometrical structures in the mixed phase. Subsequently, we have also studied kaon condensation at high-densities [24], where kaonic pasta structures appeared in the mixed phase. Through these works we have figured out the role of the Debye screening in the mixed phase.

Voskresensky et al. [25] explicitly studied the Debye screening effect for a few geometrical structures of the hadron-quark mixed phase. They have shown that the optimal value of the size of the structure cannot be obtained due to the charge screening, if the surface tension is not so small. They called it mechanical instability. It occurs because the Coulomb energy density is suppressed for the size larger than the Debye screening length (cf. Eq. (4.2)). They also suggested that the properties of the mixed phase become very similar to those given by MC, if the charge screening effectively works. The apparent violation of the Gibbs conditions in MC (Eq. (1.1)) can be remedied by including the Coulomb potential in a gauge-invariant way: the number density of charged particles is given by a gauge-invariant combination of the chemical potential and the Coulomb potential, and thereby it can be different in each phase for a constant charge chemical potential if the the Coulomb potential takes different values in both phases. However, they used a linear approximation to solve the Poisson equation analytically.

If the Coulomb interaction effect is so large, it would be important to study it without recourse to any approximation. In this paper we numerically study the charge screening effect on the structured mixed phase during the deconfinement transition in neutron-star matter in a self-consistent way. Actually we shall see importance of non-linear effects included in the Poisson equation.

3. Self-consistent calculation with the Coulomb potential

We have presented our formulation in detail in Ref. [26, 27]. Here we only briefly explain it.

We consider the geometrically structured mixed phase (SMP) where one phase is embedded in the other phase with a certain geometrical shape. We divide the whole space into equivalent charge-neutral Wigner-Seitz cells. The Wigner-Seitz cell is a representative of equally divided space under approximation of a geometrical symmetry: sphere in three dimensional (3D) case, rod in 2D case and slab in 1D case with the size R_W. The cell consists of two phases in equilibrium: one phase with a size R is embedded in the other phase as illustrated in Fig. 3.

Quark phase consists of *u*, *d*, *s* quarks and electron. We incorporate the MIT Bag model and assume the sharp boundary at the hadron-quark interface: *u* and *d* quarks are treated to be massless and *s* is massive ($m_s = 150$MeV), and they interact with each other by the one-gluon-exchange interaction inside the bag. Hadron phase consists of proton, neutron and electron. The effective potential is used to describe the interaction between nucleons and to reproduce the saturation properties of nuclear matter.

Then total thermodynamic potential (Ω_{total}) consists of the hadron, quark and electron contributions and the surface contribution:

$$\Omega_{\text{total}} = \Omega_{\text{H}} + \Omega_{\text{Q}} + \Omega_{\text{S}}, \tag{3.1}$$

where $\Omega_{\text{H(Q)}}$ denotes the contribution of hadron(quark) phase. We here introduce the surface contribution Ω_{S}, parametrized by the surface tension parameter σ, $\Omega_{\text{S}} = \sigma S$ with S being the area of the interface. Note that it may be closely related with the confining mechanism and unfortunately we have no definite idea about how to incorporate it. Actually many authors have treated its strength as a free parameter and seen how the results are changed by its value[10, 18, 20], which we also follow in this report.

To write down the thermodynamic potential we use the idea of the density functional theory (DFT) within the local density approximation (LDA) [28, 29]. The Coulomb interaction energy is included in $\Omega_{\text{H(Q)}}$ and can be expressed in terms of particle densities,

$$E_V = \frac{1}{2} \sum_{i,j} \int_{V_{\text{W}}} d^3r d^3r' \frac{Q_i \rho_i(\vec{r}) Q_j \rho_j(\vec{r}')}{|\vec{r} - \vec{r}'|}, \tag{3.2}$$

where $i = u, d, s, p, n, e$ with Q_i being the particle charge ($Q = -e < 0$ for the electron) and V_{W} the volume of Wigner-Seitz cell. Accordingly the Coulomb potential is defined as

$$V(\vec{r}) = -\sum_i \int_{V_{\text{W}}} d^3r' \frac{e Q_i \rho_i(\vec{r}')}{|\vec{r} - \vec{r}'|} + V_0, \tag{3.3}$$

where V_0 is an arbitrary constant representing the gauge degree of freedom. We fix the gauge by a condition $V(R_W) = 0$ in this paper. Operating a Laplacian ∇^2 on the Coulomb potential $V(\vec{r})$, we automatically derive the Poisson equation.

There are introduced six chemical potentials in Eq. (3.1) corresponding to particle species in the cell. Then we have to determine now eight variables, i.e., six chemical potentials, $\mu_i(i = u, d, s, p, n, e)$, and the radii R and R_W. Fixing R and R_W, we have four conditions due to chemical

equilibrium in each phase and at the interface:

$$\mu_u + \mu_e = \mu_d,$$
$$\mu_d = \mu_s,$$
$$\mu_p + \mu_e = \mu_n \equiv \mu_B,$$
$$\mu_n = \mu_u + 2\mu_d,$$
$$\left(\mu_p = 2\mu_u + \mu_d\right). \tag{3.4}$$

Therefore, once two chemical potentials μ_B and μ_e are given, we can determine other four chemical potentials, μ_u, μ_d, μ_s and μ_p. We determine μ_e by the global charge neutrality condition:

$$f_V \rho_{\mathrm{ch}}^{Q} + (1 - f_V)\rho_{\mathrm{ch}}^{H} = 0, \tag{3.5}$$

where the volume fraction $f_V = \left(\frac{R}{R_W}\right)^d$, and d denotes the dimensionality of each geometrical structure. At this point f_V is still fixed. The particle densities ρ_i are given by the equations of motion, which are derived form the extremum condition, $\frac{\delta \Omega_{\mathrm{tot}}}{\delta \rho_i} = 0$,

$$\mu_i = \frac{\delta E_{\mathrm{kin+str}}}{\delta \rho_i(\vec{r})} - N_i V(\vec{r}), \tag{3.6}$$

where $E_{\mathrm{kin+str}}$ stands for the kinetic and strong interaction energy except the Coulomb interaction energy.

Then we find the optimal value of R (R_W is fixed and thereby f_V is changed by R) by using one of GC;

$$P^{Q} = P^{H} + P_\sigma, \tag{3.7}$$

where the pressure coming from the surface tension is given by

$$P_\sigma = \sigma \frac{dS}{dV_Q}. \tag{3.8}$$

The pressure in each phase $P^{Q(H)}$ is given by the thermodynamic relation: $P^{Q(H)} = -\Omega_{Q(H)}/V_{Q(H)}$, where $\Omega_{Q(H)}$ is the thermodynamic potential in each phase and given by adding electron and the Coulomb interaction contributions to $\Omega_{Q(H)}$ in Eqs. (3.1). Finally, we determine R_W by minimizing thermodynamic potential. Thus, once μ_B is given, all other values μ_i ($i = u, d, s, p, e$) and R, R_W can be obtained. Accordingly, the particle density profiles are given by Eq. (3.6).

We numerically solve Eqs. (3.6) and the Poisson equation in a self-consistent way. In numerical calculation, every point inside the cell is represented by a grid point (the number of grid points $N_{\mathrm{grid}} \approx 100$). Equations of motion are solved by a relaxation method for a given baryon-number chemical potential under constraints of the global charge neutrality. Note that we keep GC throughout the numerical procedure.

4. Numerical results and discussions

First, we present the thermodynamic potential density of each uniform matter and that given by "bulk Gibbs" in Fig. 4. In uniform matter, hadron phase is thermodynamically favorable for
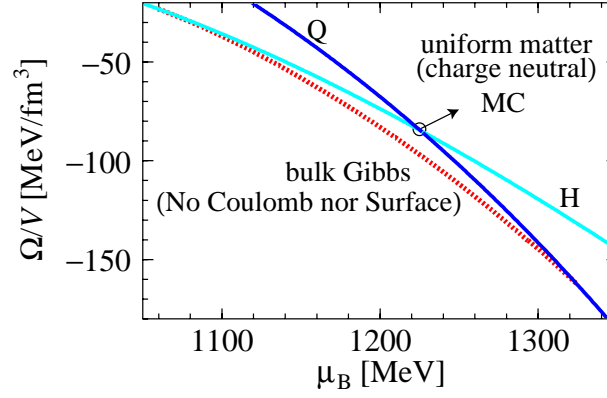
Figure 4: Thermodynamic potential density ($\Omega/V = \omega$) in the μ_B space.

$\mu_B < 1225$ MeV and quark phase above it. Therefore we plot $\delta\omega$, difference of the thermodynamic potential density between the mixed phase and each uniform matter:

$$\delta\omega = \begin{cases} \omega_{\text{total}} - \omega_H^{\text{uniform}} & \mu_B \leq 1225\text{MeV}, \\ \omega_{\text{total}} - \omega_Q^{\text{uniform}} & \mu_B \geq 1225\text{MeV}, \end{cases} \tag{4.1}$$

where $\omega_{\text{total}} = \Omega_{\text{total}}/V_W$, etc.

The results are shown in Figs. 5 and 6. In these figures we also depict two results for comparison: one is given by "bulk Gibbs", where the finite-size effects are completely discarded. The other is the thermodynamic potential given by a perturbative treatment of the Coulomb interaction, which is denoted by "no screening"; discarding the Coulomb potential $V(\vec{r})$, we solve the equations of motion to get *uniform* density profiles (no rearrangement), then evaluate the Coulomb interaction energy by using the density profiles thus determined. Note that "no screening" violates the gauge invariance, while our treatment respects it [25]. Since chemical potential itself is gauge variant, we have to include $V(\vec{r})$ together like in Eq. (3.6) to satisfy the gauge invariance: when the Coulomb potential is shifted by a constant value, $V(\vec{r}) \Longrightarrow V(\vec{r}) - V_0$, the charge chemical potential should be also shifted as $\mu_i \Longrightarrow \mu_i + N_i V_0$. Incidentally, the phase diagram in the $\mu_B - \mu_e$ plane (see, e.g., Fig. 1) is not well-defined by this reason, while many people have written it [18, 30]. We can see the screening effects by comparing the results given by "no screening" with those by the self-consistent calculation denoted by "screening". $\delta\omega$ given by MC appears as a point denoted by a circle in Figs. 5 and 6 where two conditions, $P^Q = P^H$ and $\mu_B^Q = \mu_B^H$, are satisfied. On the other hand the mixed phase derived from "bulk Gibbs" appears in a wide region of μ_B. Therefore, if the region of the mixed phase becomes narrower, it signals that the properties of the mixed phase become close to those given by MC. One may clearly see that ω_{total} becomes close to that given by MC due to the finite-size effects, the effects of the surface tension and the Coulomb interaction.

The large increase of $\delta\omega$ from the "bulk Gibbs" curve comes from the effects of the surface tension and the Coulomb potential. Since the surface tension parameter is introduced by hand, we must carefully study the effects of the surface tension and the Coulomb interaction, separately. From the difference between the result given by "no screening" and that by "bulk Gibbs", we can roughly say that about 2/3 of the increase comes from the effect of the surface tension and 1/3
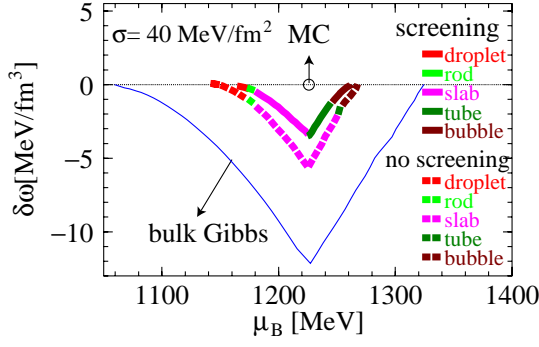
Figure 5: Difference of the thermodynamic potential density as a function of baryon-number chemical potential μ_B for $\sigma = 40\,\mathrm{MeV/fm^2}$. If $\delta\omega$ is negative, the mixed phase is a thermodynamically favorable state. MC determines one point of phase transition in uniform matter, denoted as a circle in the μ_B-$\delta\omega$ plane.
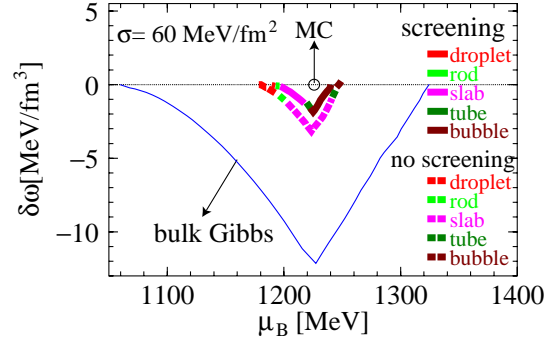
Figure 6: Same as Fig. 5 for $\sigma = 60\,\mathrm{MeV/fm^2}$. The negative $\delta\omega$ region is narrower than the $\sigma = 40\,\mathrm{MeV/fm^2}$ case.

from the Coulomb interaction (see Eq. (2.4)). Comparing the result of self-consistent calculation with that of "no screening", we can see that the change of energy caused by the screening effect is not so large , but still the same order of magnitude as that given by the surface effect.
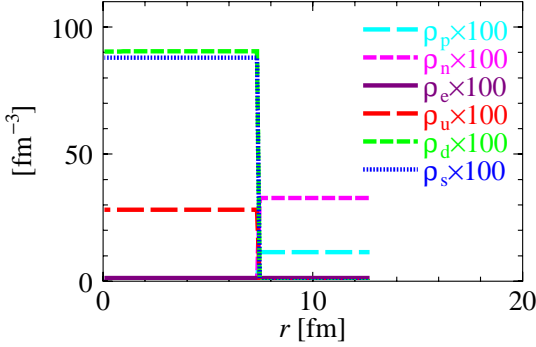
Figure 7: Density profiles in the droplet phase given by "no screening" for $\mu_B = 1189$ MeV and $\sigma = 60\,\mathrm{MeV/fm^2}$. They are uniform in each phase. $R = 7.2$ fm and $R_W = 12.8$ fm.
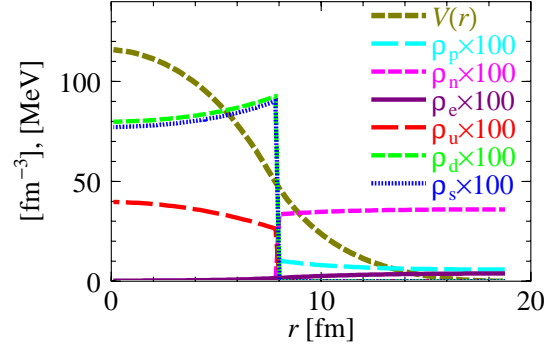
Figure 8: Density profiles and the Coulomb potential given by the self-consistent calculation for the same parameter set as Fig. 5. $R = 7.7$ fm and $R_W = 18.9$ fm.

If the surface tension is stronger, the relative importance of the charge screening effect becomes smaller and the effect of the surface tension becomes more prominent, as is seen in Figs. 5 and 6.

Although the charge screening has not so large effects on bulk properties of the matter, we shall see that it is remarkable for the charged particles to change the properties of the mixed phase. The screening effect induces the rearrangement of the charged particles. We can see this effect by comparing Fig. 7 with Fig. 8. The quark phase is negatively charged and the hadron phase is positively charged. The negatively charged particles in the quark phase such as *d*, *s*, *e* and the positively charged particle in the hadron phase *p* are attracted toward the boundary. On the

contrary the positively charged particle in the quark phase *u* and negatively charged particle in the hadron phase *e* are repelled from the boundary. The charge screening effect also reduces the net charge in each phase. In Fig. 9, we show the local charge densities of the two cases shown in Figs. 7 and 8. The change of the number of charged particles due to the screening is as follows: In the quark phase, the numbers of *d* and *s* quarks and electrons decrease, while the number of *u* quark increases. In the hadron phase, on the other hand, the proton number should decrease and the electron number should increase. Consequently the local charge decreases in the both phases.

In Fig. 9 we can see that the core region of the droplet tends to be charge-neutral and near the boundary of the Wigner-Seitz cell is almost charge-neutral. In Figs. 10 and 11 we present the lump and cell radii for each density. As we have shown in the previous paper[25], the Coulomb energy is suppressed for larger *R* by the screening effect. The *R* dependence of the total thermodynamic potential comes from the contributions of the surface tension and the Coulomb interaction: the optimal radius giving the minimum of the thermodynamic potential is then determined by the balance between two contributions, since the former gives a decreasing function, while the latter an increasing one. If the Coulomb energy is suppressed, the minimum of the thermodynamic potential is shifted to larger radius. As a result the size of the embedded phase (*R*) and the cell size (R_W) become large. In Ref. [25] they demonstrated that the minimum

Figure 9: Local-charge densities for the 'no screening' case and the case of the self-consistent with the screening effect. For 'no screening', charge density of each phase is constant over the region. The absolute value of the charge density is larger than that given by the self-consistent calculation in each phase. In the hadron phase, the charge density becomes almost vanished near the cell boundary $r = R_W$.

disappears for a large value of the surface tension parameter: the structure becomes mechanically unstable in this case.

We cannot show it directly in our framework because such unstable solutions are automatically excluded during the numerical procedure, while we can see its tendency in Figs. 10 and 11: *R* and R_W get larger by the screening effect.

We also see the relation between the size of the geometrical structure and the Debye screening length. The Debye screening length appears in the *linearized* Poisson equation and is then given as

$$(\lambda_D^q)^{-2} = 4\pi \sum_f Q_f \left(\frac{\partial \langle \rho_f^{\mathrm{ch}} \rangle}{\partial \mu_f} \right), \quad (\lambda_D^p)^{-2} = 4\pi Q_p \left(\frac{\partial \langle \rho_p^{\mathrm{ch}} \rangle}{\partial \mu_p} \right), \quad (\lambda_D^e)^{-2} = 4\pi Q_e \left(\frac{\partial \langle \rho_e^{\mathrm{ch}} \rangle}{\partial \mu_e} \right), \quad (4.2)$$

where $\langle \rho_f^{\mathrm{ch}} \rangle$ stands for the averaged density in quark phase, $\langle \rho_p^{\mathrm{ch}} \rangle$ is proton number averaged density in the hadron phase and $\langle \rho_e^{\mathrm{ch}} \rangle$ is the electron charge density averaged inside the cell. It gives a rough measure for the screening effect: At a distance larger than the Debye screening length, the Coulomb interaction is effectively suppressed.

In Fig. 10 we show sizes of geometrical structure for "no screening" case. If we ignore the screening effect, the size of the embedded phase is comparable or smaller than the corresponding
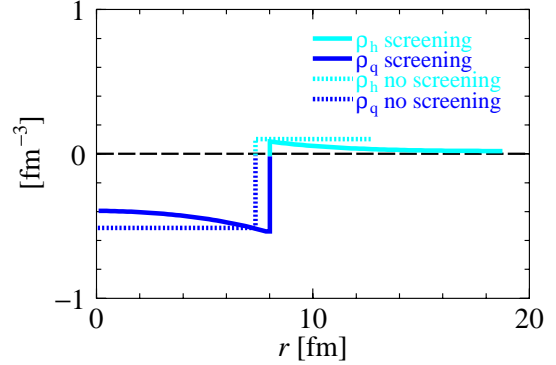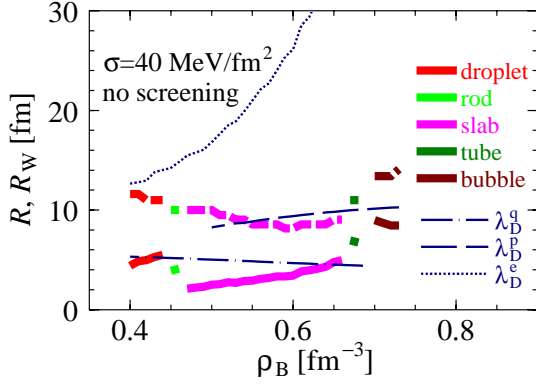
Figure 10: Lump and cell radii given by the 'no screening' calculation. The Debye screening length is also depicted for comparison. R is thick-solid line and R_W is thick-dashed line. We can see the size of the structure becomes less than the Debye screening length.
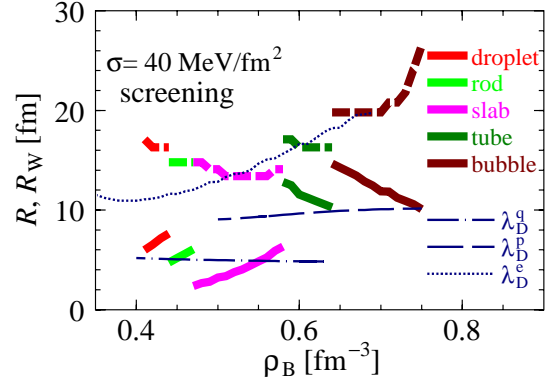
Figure 11: Same as Fig. 10 given by the self-consistent calculation with the screening effect. The size of the structure becomes larger than that given by 'no screening', and consequently exceeds the Debye screening length.
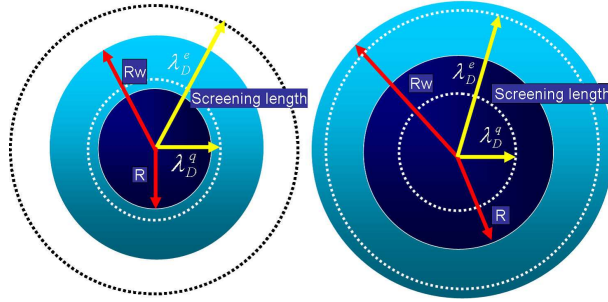

Figure 12: Schematic graphs of the droplet size and the Debye screening length. Right figure shows the case of the self-consistent calculation with the screening effect and left figure 'no screening'.

quark Debye screening length λ_D^q (Fig. 12). This may mean that the Debye screening is not so important. Actually, many authors have neglected the screening effect due to this argument[18, 20]. In Fig. 11, however, we see that the size of the embedded phase can be larger than λ_D^q (Fig. 12) in the self-consistent calculation. We can also see the similar situation about R_W and λ_D^e. This means that the screening has important effects in this mixed phase. We cannot expect such a effect without solving the Poisson equation because of the non-linearity.

We present EOS in Figs. 13 and 14. We can see that EOS of two cases become close to that given by MC by including the finite size effects. Moreover, EOS of "screening" becomes more similar to that given by MC than that of "no screening". We show the pressure results in Figs. 15 and 16, which is given by $P = \rho_B^2 \frac{\partial (E/N_B)}{\partial \rho_B}$ or $P = -\Omega/V$: the former is given by using Figs. 13 and 14 and the latter by using the results of Fig. 5. The pressure becomes more similar to that given by MC by the charge screening effect, which shows a larger pressure near the beginning and weaker one near the termination of the phase transition.

We have used the surface tension parameter σ in the present study. Surface tension is a very
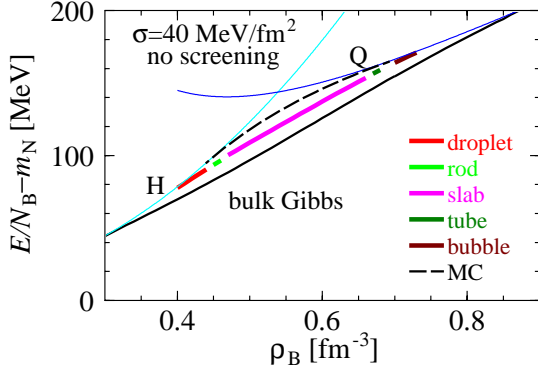
Figure 13: Equation of state for $\sigma = 40$ MeV/fm^2 without screening effect.
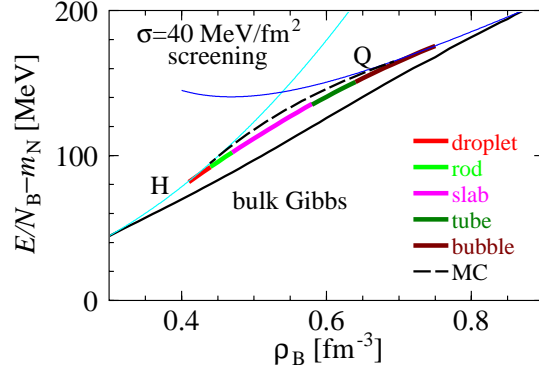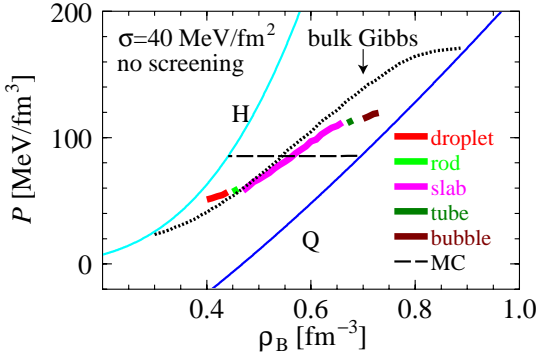
Figure 14: Same as Fig. 13 for 'screening'.

Figure 15: Pressure as a function of baryon-number density given by the 'no screening' calculation for $\sigma = 40$MeV/fm^2. The results given by 'bulk Gibbs' and MC are also presented for comparison.
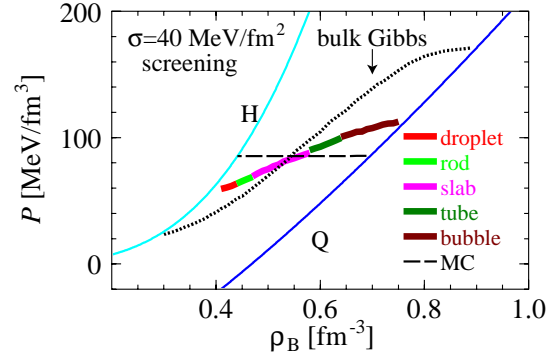
Figure 16: Same as Fig. 15 given by the self-consistent calculation with the screening effect.

difficult problem because it should be self-consistent with the two phases of matter, quark and hadron. Lattice QCD, based on the first principle, predicts that σ may be 10-100 MeV/fm^2[31, 32]. Although this result is for high temperature case, our choice is within it. Moreover, the results given by other model calculations [33, 34, 35, 36] are similar to our value.

Let us briefly consider some implication of these our results for compact star phenomena. Glendenning[10] suggested many SMP appear in the core region by using "bulk Gibbs": the mixed phase should appear for several kilometers. However we can say that the region of SMP should be narrow in the μ_B space and EOS is more similar to that of MC due to the finite-size effects. These results look to be consistent with those given by other studies. Bejger et al. [37] have examined the relation between the mixed phase and glitch phenomena, and shown that the mixed phase should be narrow if the glitch is generated by the mixed phase in the inner core. On the other hand the gravitational wave asks for density discontinuity in the core region[38].

5. Summary and concluding remarks

We have studied the charge screening effect in the hadron-quark mixed phase in neutron-star matter. We have elucidated the charge screening effect comparing the results of "no screening" with those of "screening" which includes non-linearity of the Poisson equation. The density profiles of the charged particles are drastically modified by the screening effect, while the thermodynamic potential is not affected so much; the charge rearrangement induced by the screening effect tends to make the net charge smaller in each phase. Consequently the system tends to be locally charge-neutral, which suggests that the Maxwell construction (MC) is effectively justified even if it is thermodynamically incorrect. In this context, it would be interesting to refer to the work by Heiselberg [39], who studied the screening effect on a quark droplet (strangelet) in the vacuum, and suggested the importance of the rearrangement of charged particles.

We have seen that thermodynamic quantities such as thermodynamic potential and energy become close to those derived from MC by the screening effect, which also suggests that MC is effectively justified due to the screening effect. As another case of the system with two or more chemical potentials, kaon condensation has been also studied [23] and the results are shown to be similar to those in the present study. Thus the importance of the screening effect should be a common feature for the first-order phase transitions in high-density matter.

We have included the surface tension at the hadron-quark interface, while its definite value is not clear at present. An uncertainty in the value of the surface tension does not allow to conclude whether the mixed phase exists or not. There are many estimations for the surface tension at the hadron-quark interface in lattice QCD [31, 32], in shell-model calculations [33, 34, 35] and in model calculations based on the dual-Ginzburg Landau theory [36]. Our parameter is in that reasonable range.

We have considered some implications of our results for neutron star phenomena. The screening effect would restrict the allowed region of the structured mixed phase in neutron stars, in contrast with a wide region given by "bulk Gibbs"[10, 21]. It could be said that they should change the bulk property of neutron stars, especially the structure of the core region.

Compact stars have the strong magnetic field and its origin is not well understood. One possibility is that it comes from ferromagnetism of the quark matter in the core [40, 41, 42]. Therefore it should be interesting to include the magnetic field contribution in our formalism. We have assumed zero temperature here. It would be much interesting to include the finite-temperature effect. Then it is possible to draw the phase diagram in the μ_B - T plane and we can study the properties of the deconfinement phase transition; our study may be extended to treat the mixed phase to appear during the hadronization of QGP in the nucleus-nucleus collisions and supernova explosions.

In this study we have used a simple model for quark matter to figure out the finite-size effects in SMP. However, it has been suggested that the color superconductivity would be a ground state of quark matter [18, 43, 44]. Hence we will include it in a further study. The hadron phase should be also treated more realistically; for example, we should include the hyperons or kaons in hadron matter. In the recent studies the mixed phase has been also studied [45, 46, 47] in the context of various phases in the color superconducting phase.

Acknowledgements

References

[1] K. Adcox et al. (PHENIX collaboration), Phys. Rev. Lett. **88** (2002) 022301; C. Adler et al. (STAR collaboration), Phys. Rev. Lett. **90** (2003) 082302

[2] J. Madsen, Lect. Notes Phys. **516** (1999) 162

[3] K. S. Cheng, Z. G. Dai and T. Lu, Int. Mod. Phys. D**7** (1998) 139

[4] For review, D. H. Rischke, Prog. Part. Nucl. Phys. **52** (2004) 197; J. Macher and J. Schaffner-Bielich, Eur. J. Phys. **26** (2005) 341 and references therein.

[5] R. D. Pisalski and F. Wilczek, Phys. Rev. Lett. **29** (1984) 338

[6] R. V. Gavai, J. Potvin and S. Sanielevici, Phys. Rev. Lett. **58** (1987) 2519

[7] Y. A. Terasov, Phys. Rev. C **70** (2004) 054904

[8] S. Pratt and S. Pal, Phys. Rev. C **71** (2005) 014905

[9] J. M. Peters and K. L. Haglin J. Phys. G: Nucl. Part. Phys.31 (2005) 49

[10] N. K. Glendenning and S. Pei, Phys. Rev. C **D52** (1995) 2250

[11] F. Weber, Prog. Part. Nucl. Phys. **54** (2005) 193

[12] F. Weber, J. Phys. **G25** (1999) R195

[13] N. K. Glendenning, Phys. Rev. D **D46** (1992) 1274; Phys. Rep. **342** (2001) 393.

[14] W. Weise, and G. E. Brown, Phys. Lett. B **58** (1975) 300

[15] A. B. Migdal, A. I. Chernoustan and I. N. Mishustin, Phys. Lett. B **83** (1979) 158

[16] J. Ellis, J. Kapusta and K. A. Olive, Nucl. Phys. B **348** (1991) 345

[17] A. Rosenhauer, E. F. Staubo, L. P. Csernai, T. Øvergård, and E. Østgaad, Nucl. Phys. A **540** (1992) 630

[18] M. Alford, K. Rajagopal, S. Reddy, and F. Wilczek, Phys. Rev. D **64** (2001) 074017

[19] T. Endo, Toshiki Maruyama, S. Chiba and T. Tatsumi, Nucl. Phys. A **749** (2005) 333c

[20] H. Heiselberg, C. J. Pethick and E. F. Staubo, Phys. Rev. Lett. **70** (1993) 1355

[21] N. K. Glendenning, *Compact stars*, Springer 2000.

[22] T. Norsen and S. Reddy, Phys. Rev. C. **63** (2001) 065804

[23] Toshiki Maruyama, T. Tatsumi, D. N. Voskresensky, T. Tanigawa and S. Chiba, Nucl. Phys. A **749** (2005) 186c; Phys. Rev C **72** (2005) 015802

[24] Toshiki Maruyama, T. Tatsumi, D. N. Voskresensky, T. Tanigawa, T. Endo and S. Chiba, nucl-th/0505063

[25] D. N. Voskresensky, M. Yasuhira and T. Tatsumi, Phys. Lett. **B541** (2002) 93, ; Nucl. Phys. **A723** (2003) 291; T. Tatsumi, M. Yasuhira and D. N. Voskresensky, Nucl. Phys. **A718** (2003) 359c; T. Tatsumi and D. N. Voskresensky, nucl-th/0312114.

[26] T. Endo, Toshiki Maruyama, S. Chiba and T. Tatsumi, hep-ph/0502216

[27] T. Endo, Toshiki Maruyama, S. Chiba and T. Tatsumi, hep-ph/0510279

[28] R. G. Parr and W. Yang, *Density-Functional Theory of atoms and molecules*, Oxford Univ. Press, 1989.

[29] E. K. U. Gross and R. M. Dreizler, *Density functional theory*, Plenum Press (1995)

[30] N. K. Glendenning and J. Schaffner-Bielich, Phys. Rev. C **60** (2000) 025803

[31] K. Kajantie, L. Kärkäinen, and K. Rummukainen, Nucl. Phys. **B357** (1991) 693

[32] S. Huang, J. Potvion, C. Rebbi and S. Sanielevici, Phys. Rev. D **43** (1991) 2056

[33] J. Madsen, Phys. Rev. D **46** (1992) 329

[34] J. Madsen, Phys. Rev. Lett. **70** (1993) 391

[35] M. S. Berger and R. L. Jaffe, Phys. Rev. C **35** (1987) 213

[36] H. Monden, H. Ichie, H. Suganuma and H. Toki, Phys. Rev. C **57** (1998) 2564

[37] M. Bejger, P. Haensel and J. L. Zdunik, Mon. Not. Roy. Astron. Soc. **359** (2005) 699

[38] G. Miniutti, J. A. Pons, E. Berti, L. Gualtieri, V. Ferrari, Mon. Not. Roy. Astron. Soc. **338** (2003) 389

[39] H. Heiselberg, Phys.Rev.D. **48** (1993) 1418

[40] T. Tatsumi, T. Maruyama and E. Nakano, Prog. Theor. Phys. Suppl. **153** (2004) 190

[41] E. Nakano, T. Maruyama and T. Tatsumi, Phys. Rev. D **68** (2003) 105001

[42] T. Tatsumi, Phys. Lett. B **489** (2000) 280

[43] M. Alford, K. Rajagopal and F. Wilczek, Nucl. Phys. B **64** (1999) 443, D. Bailin and A. Love, Phys. Rep. **107** (1984) 325. As resent reviews, M. Alford, hep-ph/0102047; K. Rajagopal and F. Wilczek, hep-ph/0011333

[44] M. Alford and S. Reddy, Phys. Rev. D **67** (2003) 074024

[45] F. Neumann, M. Buballa and M. Oertel Nucl. Phys. A **714** (2003) 481

[46] I. Shovkovy, M. Hanauske and M. Huang, Phys. Rev. D **67** (2003) 103004

[47] S. Reddy and G. Rupak, Phys. Rev. D **71** (2005) 025201